PHYSICAL REVIEW C **78**, 031302(R) (2008)

Lifetime measurement of candidate chiral doublet bands in the ^{103,104}Rh isotopes with the recoil-distance Doppler-shift method in inverse kinematics

T. Suzuki,[1,2,*] G. Rainovski,[3,4] T. Koike,[2] T. Ahn,[4] M. P. Carpenter,[5] A. Costin,[4] M. Danchev,[6] A. Dewald,[7] R. V. F. Janssens,[5] P. Joshi,[8] C. J. Lister,[5] O. Möller,[7,9] N. Pietralla,[4,9] T. Shinozuka,[1] J. Timár,[10] R. Wadsworth,[8] C. Vaman,[11] and S. Zhu[5]

[1]*Cyclotron and Radio-isotope Center, Tohoku University, Sendai 980-8578, Japan*
[2]*Department of Physics, Tohoku University, Sendai 980-8577, Japan*
[3]*St. Kliment Ohridski University of Sofia, Sofia 1164, Bulgaria*
[4]*Department of Physics and Astronomy, SUNY, Stony Brook, New York 11794-3800, USA*
[5]*Physics Division, Argonne National Laboratory, Argonne, Illinois 60439, USA*
[6]*Department of Physics, University of Tennessee Knoxville, Tennessee 37996, USA*
[7]*Institute für Kernphysik der Universität zu Köln, D-50937 Köln, Germany*
[8]*Department of Physics, University of York, Heslington YO10 5DD, United Kingdom*
[9]*Institut für Kernphysik, TU Darmstadt, D-64689, Darmstadt, Germany*
[10]*Institute of Nuclear Research (ATOMKI), Pf. 51, 4001 Debrecen, Hungary*
[11]*National Superconducting Cyclotron Laboratory, Michigan State University, East Lansing, Michigan 48824, USA*

(Received 30 July 2008; published 22 September 2008)

Lifetimes of chiral candidate structures in ^{103,104}Rh were measured using the recoil distance Doppler-shift method. The Gammasphere detector array was used in conjunction with the Cologne plunger device. Excited states of ^{103,104}Rh were populated by the ^{11}B(^{96}Zr, $4n$)^{103}Rh and ^{11}B(^{96}Zr, $3n$)^{104}Rh fusion-evaporation reactions in inverse kinematics. Three and five lifetimes of levels belonging to the proposed chiral doublet bands are measured in ^{103}Rh and ^{104}Rh, respectively. The previously observed even-odd spin dependence of the $B(M1)/B(E2)$ values is caused by the variation in the $B(E2)$ values, whereas the $B(M1)$ values decrease as a function of spin.

DOI: 10.1103/PhysRevC.78.031302 PACS number(s): 21.10.Tg, 21.10.Re, 27.60.+j

Nuclear chirality is the most recently recognized form of spontaneous symmetry breaking in nuclei [1]. Mutually orthogonal coupling of three angular momenta results in the formation of either left- or right-handed geometry in the body-fixed frame and leads to a doubling of states in the laboratory frame. The two systems are related via time reversal rather than parity transformation, thereby making nuclear chirality unique among other chiralities observed in a wide scale range of nature from elementary particles to biological systems such as human hands. In nuclei, stable triaxial deformation is essential for the mutual perpendicular coupling of the angular momenta involved.

Nearly degenerate pairs of $\Delta I = 1$ rotational bands, which are interpreted as a manifestation of chirality, are observed systematically in several odd-odd and in a few odd-A nuclei in the mass $A \sim 130$ [2–9] and the $A \sim 100$ [10–14] regions. In these odd-odd nuclei, three angular momenta are provided by the valence proton, valence neutron, and the core rotation that align along the respective three principal axes of the triaxially deformed core to minimize the energy of the nuclear system. In odd-A nuclei, chiral bands are built on the three quasiparticle configuration in which a broken pair of nucleons provides one of the three angular momenta.

Observation of chiral doublet bands demands an experimental verification of identical properties between the doublet members. Therefore, two experimental criteria must be fulfilled; (i) the observation of nearly degenerate $\Delta I = 1$ bands built on the same single-particle configuration and (ii) identical electromagnetic properties, namely similar $B(E2)$ and $B(M1)$ values of in-band and interband transitions. In addition, as a consistency check for the perpendicular coupling of single particle angular momenta and the core rotation, constancy of $S(I) = [E(I) - E(I-1)]/2I$ as a function of spin, is expected.

Early studies have concentrated on the criterion (i) and identified the chiral doublet candidates. However, the more stringent test (ii) has been pursued with lifetime measurements of ^{134}pr [15], ^{132}La, ^{128}Cs [16], and ^{135}Nd [17] in the mass $A \sim 130$ region. The results for ^{134}Pr, of which the doublet structures exhibit the best overall energy degeneracy, revealed similar $B(M1)$ values, but 2–3 times larger $B(E2)$ values for the main band compared to its partner. This in turn led to the chiral interpretation of the doublet bands observed being questioned [18]. The latest lifetime measurement in odd-A ^{135}Nd, however, reported nearly the same $B(E2)$ and $B(M1)$ values for the doublet states [17].

In the mass $A \sim 100$ region, chiral doublet structures are expected for the $\pi g_{9/2}{}^{-1} \otimes \nu h_{11/2}$ configuration in odd-odd nuclei and for the $\pi g_{9/2}{}^{-1} \otimes \nu h_{11/2}{}^{2}$ configuration in odd-A nuclei. The odd-A and odd-odd nuclei, ^{103,104}Rh are considered as promising candidates in this mass region [10,14].

The doublet bands in ^{103}Rh and ^{104}Rh are built on three- and two-quasiparticle configurations, respectively. The doublet structure in ^{104}Rh was first identified at SUNY at Stony Brook and studied further at LBNL using Gammasphere with the ^{96}Zr(^{11}B, $3n$) reaction. The high sensitivity of the latter experiment allowed for the identification of the doublet structures

*tomokazu@rcnp.osaka-u.ac.jp; Research Center for Nuclear Physics, Osaka University, Mihogaoka, Ibaraki, Osaka, 567-0047, Japan.

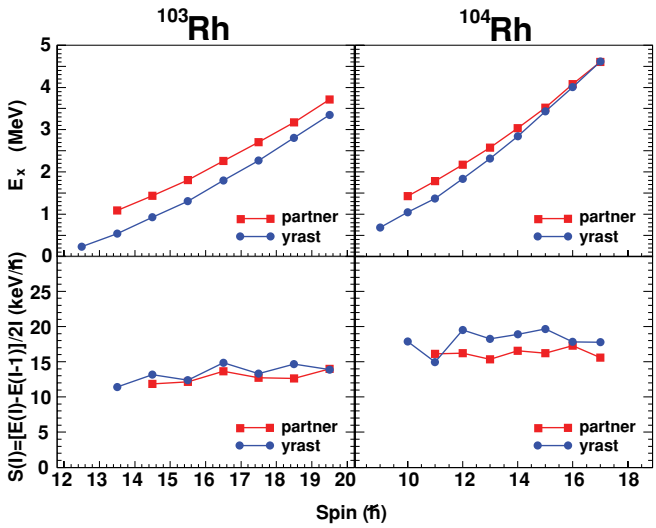

FIG. 1. (Color online) Excitation energy (upper) and $S(I) = [E(I) - E(I-1)]/2I$ values (lower) as a function of spin for the chiral candidate bands of ^{103}Rh (left) and ^{104}Rh (right).

in ^{103}Rh corresponding to the $4n$ evaporation channel. A three quasiparticle configuration of ^{103}Rh, $\pi {g_{9/2}}^{-1} \otimes \nu {h_{11/2}}^2$ was assigned in Ref. [19] for the bands with the band head at $I = \frac{23}{2}$. The energy degeneracy is less than 400 keV over the entire spin range.

The energy separation and $S(I)$ values for ^{103,104}Rh are shown in Fig. 1. The near constancy of the $S(I)$ values for both ^{103,104}Rh indicates weak Coriolis interactions resulting from perpendicular angular momenta coupling of the single particle to that of the core. Systematic observation of the doublet bands in ^{102,103,104,105}Rh isotopes were discussed in Ref. [14]. ^{102,104}Rh or ^{103,105}Rh isotopic combinations have different cores, namely ^{100}Ru and ^{102}Ru, respectively, but the doublets are built on the same single quasiparticle configuration. However, the ^{102,103}Rh and ^{104,105}Rh combinations have the same core but different single-particle configurations. In terms of energy degeneracy, the latter combinations show almost identical behavior within the paired isotopes, indicating the strong influence of the core rather than the valence particles on the degeneracy.

In the present work, lifetimes of chiral doublet members in the ^{103,104}Rh isotopic chain were measured in a single experiment. This is the first such measurement in this mass region.

High-spin states in ^{103,104}Rh were populated using inverse kinematics via the ^{11}B(^{96}Zr, xn) reaction, where $x = 4, 3$, respectively, at a beam energy of 330 MeV. The beam was provided by Argonne Tandem Linear Accelerator System. Lifetimes of excited states were measured using the recoil distance Doppler-shift (RDDS) method with the Cologne plunger device [20], which was mounted inside Gammasphere. The array consisted of 101 Compton-suppressed Ge detectors for detection of the emitted γ rays. The target used, especially developed for this experiment [21], was 300 μg/cm^2 ^{11}B, deposited on a 4-mg/cm^2 ^{93}Nb foil. A mean measured recoil velocity of ^{103,104}Rh after the Nb-backed target was $\beta = 5.1(1)\%$ and $5.7(3)\%$, respectively. The large recoil velocities obtained by the use of the inverse kinematics reaction in the present experiment allow for a measurement of lifetimes shorter than 1 ps. However, stopping the recoils without producing sizable Doppler attenuation effects is not possible. Therefore, a degrader foil of 3.5-mg/cm^2-thick ^{93}Nb was used in the Cologne plunger device, instead of the usual stopper foil. The degrader decreases the recoil velocity to $\beta = 3.1(1)\%$ and $3.3(2)\%$ for ^{103,104}Rh, respectively. Moreover, the thickness of the target and the degrader foils are chosen so that the transit time of the recoils in these materials does not exceed 0.2 ps to minimize the target/degrader related smearing of the Doppler shifts, whereas the expected lifetimes for the levels of interest are on the order of 1 ps. Seven target-degrader distances ranging from 8 to 100 μm were used for the measurement. Twofold or higher Compton suppressed γ coincidence events were collected. For each distance, on average, a total of approximately 4×10^8 unfolded events were recorded and sorted into γ-γ matrices.

The differential decay-curve method (DDCM) [22] was used for the data analysis. The lifetime τ of the level of interest is obtained from

$$\tau = \frac{I_{s,u}^{\mathrm{BA}}(x)}{I_{s,s}^{\mathrm{BA}}(x+\Delta x) - I_{s,s}^{\mathrm{BA}}(x-\Delta x)} \frac{2\Delta x}{v}, \qquad (1)$$

where v is the recoil velocity and Δx is the difference between the two target-degrader distances. $I_{s,u}^{\mathrm{BA}}$ is the peak area of the Doppler unshifted (u) components of a depopulating transition A in coincidence with the shifted (s) component of the directly feeding transition B. The denominator is the difference of the s components between the two distances, that is, the number of in-flight decay events over the flight time $2\Delta x/v$. The fitted peak areas measured at three different distances at x and $x \pm \Delta x$ were normalized to intense transitions in each nucleus. When the directly feeding transition B is contaminated and cannot be used as a gate, any other transition above, C, which is also coincidence with A, was used instead. Then the lifetime can be obtained by

$$\tau = \frac{I_{s,u}^{\mathrm{CA}}(x) - \alpha I_{s,u}^{\mathrm{CB}}(x)}{I_{s,s}^{\mathrm{CA}}(x+\Delta x) - I_{s,s}^{\mathrm{CA}}(x-\Delta x)} \frac{2\Delta x}{v}, \quad \alpha = \frac{I^{\mathrm{CA}}}{I^{\mathrm{CB}}}, \qquad (2)$$

where α is the ratio of intensity of the peaks A and B in a coincidence spectrum gated on C.

For the lifetime extraction, the detectors placed in the forward and the backward directions were grouped into seven rings that were located at the polar angles of 35° (combination of detectors positioned at 32° and 37°), 50°, 58°, 122°, 130°, 146° (combination at 143° and 148°), and 163° with respect to the beam axis. The γ-γ matrices for all possible ring combinations were sorted and analyzed. Middle-ring detectors (60° $\sim$ 120°) were not sufficiently sensitive to the Doppler shifts and were used only as cleaning gates in the analysis of ^{104}Rh and were not used in the analysis of ^{103}Rh due to low statistics. Typical RDDS spectra are provided in Fig. 2, in which the Doppler-shift correction was applied such that the unshifted peak component is shifted back to

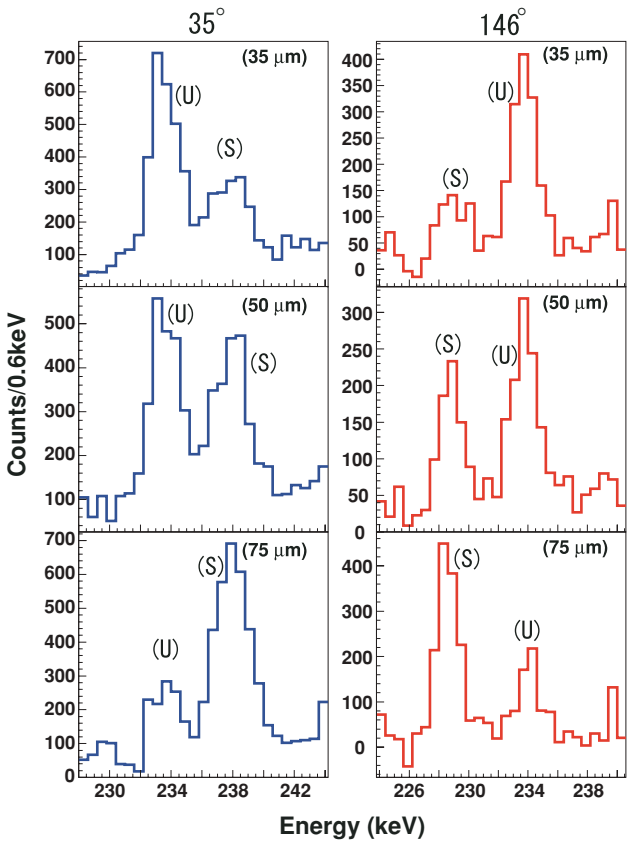

FIG. 2. (Color online) Background-subtracted spectra of the 234-keV peak in ^{103}Rh, obtained by gating on the shifted components of the 382+384-keV transition for three different target-degrader distances as seen in the rings of $\theta = 35^\circ$ (left) and $\theta = 146^\circ$ (right). Shifted and unshifted components are marked as (S) and (U), respectively.

the original energy. The extracted lifetimes are listed in Tables I and II for ^{103}Rh and for ^{104}Rh, respectively.

Reduced transition probabilities were deduced from the measured lifetimes in the present work and are tabulated in Table III. The energies and branching ratios of corresponding levels are adopted from the previous experimental data [10,14]. The $B(M1; I \rightarrow I-1)$ values were obtained by assuming pure $M1$ multipolarity. The quoted uncertainties were determined from transition energies, branching ratios, and lifetimes.

TABLE I. Extracted lifetimes in ^{103}Rh. The same band numbering as in Ref. [14] are used. Three levels measured in Band 3 are chiral doublet candidates. Lifetimes with star(∗) are obtained using Eq. (2).

Band	I^π ($\hbar$)	E_γ (keV)	τ (ps)	
Band 1	$\frac{13}{2}^+$	728	4.3 ± 1.9	∗
	$\frac{17}{2}^+$	895	0.78 ± 0.18	∗
	$\frac{21}{2}^+$	1022	0.72 ± 0.13	∗
Band 3	$\frac{23}{2}^+$	659	0.99 ± 0.27	
	$\frac{25}{2}^+$	234	0.95 ± 0.17	∗
	$\frac{27}{2}^+$	382	1.0 ± 0.1	∗
	$\frac{29}{2}^+$	384	0.72 ± 0.23	

TABLE II. Extracted lifetimes in ^{104}Rh.

I^π ($\hbar$)	E_γ (keV)	τ (ps)
9^-	158	6.21 ± 0.45
10^-	357	1.25 ± 0.09
11^-	328	1.34 ± 0.12
12^-	468	1.05 ± 0.10
13^-	475	0.71 ± 0.19

The measured $B(E2)$ and $B(M1)$ values as a function of spin for ^{103,104}Rh are given in Fig. 3. Seven lifetimes are extracted for ^{103}Rh, and those three that are related to the doublet bands are discussed here. The behavior as well as absolute values of the $B(E2)$ and $B(M1)$ between the two nuclei are similar; the $B(E2)$ values exhibit weak staggering, whereas the $B(M1)$ values decrease monotonically with increasing spin. Therefore, we conclude that the $B(M1)/B(E2)$ staggering observed in the previous experiments is caused by the $B(E2)$ rather than $B(M1)$ values. The observed band-head spin of the $\pi {g_{9/2}}^{-1} \otimes \nu {h_{11/2}}^2$ configuration in ^{103}Rh and of the $\pi {g_{9/2}}^{-1} \otimes \nu h_{11/2}$ configuration in ^{104}Rh is $\frac{23}{2}$ and 8, respectively. These values are close to those obtained when the angular momenta of a valence protons and neutrons are coupled perpendicularly and added semiclassically.

The decreasing $B(M1)$ values are interesting and need theoretical interpretation. Recent particle rotor calculations [23] for the isotone, ^{106}Rh predict the decreasing $B(M1)$ values as well as effective angle between the valence proton and neutron as a function of spin. The two single-particle angular momenta are coupled perpendicularly at the band head. The coupling angle decreases to $\sim 45^\circ$ at $I = 16$, where the rotation is still aplanar, having nonzero effective angles of $\sim 60^\circ$ between the respective valence nucleons and the collective core. Other possible causes may be attributed to a shape change and its coupling to the single-particle degree of freedom.

One of the common features of the observed doublet bands is the odd-even spin staggering of $B(M1)/B(E2)$ values. In

TABLE III. Extracted $B(E2)$ and $B(M1)$ values in the chiral candidates in ^{103}Rh and ^{104}Rh. Band numbers are the same as those in Table I.

Nuclei/band	States (I^π)	$B(M1)(\mu_N{}^2)$	$B(E2)(e^2\mathrm{b}^2)$
^{103}Rh	$\frac{25}{2}^+$	2.3(4)	0.077(14)
(Band 3)	$\frac{27}{2}^+$	1.8(2)	0.14(3)
	$\frac{29}{2}^+$	1.2(4)	0.11(4)
^{104}Rh	9^-	2.3(2)	
	10^-	0.95(8)	0.063(17)
	11^-	0.91(12)	0.093(20)
	12^-	0.44(6)	0.039(10)
	13^-	0.42(15)	0.067(25)

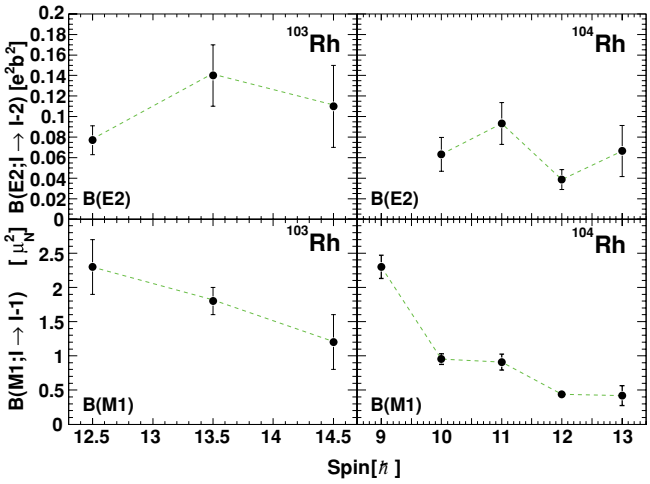

FIG. 3. (Color online) Experimentally determined $B(E2)$ and $B(M1)$ reduced transition probabilities in the chiral candidates in ^{103,104}Rh. The dashed lines between the data points are drawn to guide the eye.

both the mass $A \sim 130$ and $A \sim 100$ regions, the staggering pattern in odd-odd nuclei is that the ratios are small for $I - I_0 =$ odd and large for $I - I_0 =$ even where I_0 is a band-head spin. For the $\pi h_{11/2} \otimes \nu {h_{11/2}}^{-1}$ configuration, $I_0 = 9$ [3] is adopted and for the $\pi g_{9/2} \otimes \nu {h_{11/2}}^{-1}$ configuration $I_0 = 8$. Among the odd-A nuclei, the doublet bands observed in the $A \sim 130$ region is only one, namely ^{135}Nd with the $\pi h_{11/2} \otimes \nu {h_{11/2}}^{-2}$ configuration. The staggering in the $B(M1)/B(E2)$ ratio is also seen; the ratio is small for $I - I_0 =$ odd and large for $I - I_0 =$ even. The band-head spin is $I_0 = \frac{25}{2}$. This dependence of staggering on spin is the same for the $\pi {g_{9/2}}^{-1} \otimes \nu {h_{11/2}}^{2}$ configuration in the mass $A \sim 100$ region where $I_0 = \frac{23}{2}$. The staggering patterns are summarized in Table IV. For the mass $A \sim 130$ region, the absolute $B(M1)$ and $B(E2)$ values are measured for the odd-odd ^{128}Cs [16] and the odd-A ^{135}Nd nuclei. In both cases, the staggering is caused by the $B(M1)$ values. It should be noted, however, that, in the case of ^{128}Cs, the $B(E2)$ staggering has the opposite phase to that of the $B(M1)$ staggering. The phase of the absolute $B(E2)$ values is the same between ^{128}Cs and ^{104}Rh. These staggering patterns are summarized in Table V. Particle rotor model calculations for the $\pi h_{11/2} \otimes \nu h_{11/2}$ configuration with $\gamma = 30^\circ$ [24] and for the $\pi g_{9/2} \otimes \nu h_{11/2}$ configuration in ^{106}Rh [23] predict an odd-even spin dependence of the $B(M1)$ values at higher spins where the chiral geometry is well defined with a sufficiently developed core angular momentum, whereas $B(E2)$ values are void of such dependence over the entire spin range. Similar calculations for ^{104}Rh are highly desirable to compare with the present results. On the experimental side, the measurement should be extended to the higher-spin states and to the side-band states.

TABLE V. Odd-even spin dependence of the absolute $B(M1)$ and $B(E2)$ values.

$I - I_0$	$B(E2)$		$B(M1)$		Ref.
	Even	Odd	Even	Odd	
^{128}Cs	Small	Large	Large	Small	[16]
^{104}Rh	Small	Large	None	None	
^{135}Nd	None	None	Small	Large	[17]
^{103}Rh	Small	Large	None	None	

In summary, the lifetimes of three and five levels at the bottom of the three- and two-quasiparticle bands in ^{103}Rh and ^{104}Rh, respectively, have been measured via the recoil distance Doppler-shift method. The DDC method was used for the analysis. These are the first measurements in this mass region for a pair of bands considered as chiral doublets. The behavior of the $B(E2)$ and $B(M1)$ values in both nuclei is similar; the $B(E2)$ values exhibit an odd-even spin dependence and the $B(M1)$ values decrease with increasing spin. Therefore, the staggering observed in $B(M1)/B(E2)$ ratios is caused by the $B(E2)$ values. This result is unique and different from that for other chiral doublet candidates in the mass $A \sim 130$ region. The staggering in the $B(E2)$ values, but not in the $B(M1)$ values, is not yet understood and demands theoretical interpretation. At the same time, it is absolutely necessary to measure the lifetimes of levels at higher spin together with those for the yrare partner band where the energy degeneracy is good. If the $B(E2)$ and $B(M1)$ values of the partner bands are similar and thus exhibit the same behaviors, this gives a strong support for these bands to be chiral partners because of their surprising band properties regardless of their origin. Or if the electromagnetic properties of the two bands are diffident at low spins, but get closer at higher spins with the energy degeneracy, they can be seen as transitioning to chiral rotation at the higher spins. However, if none of the above is observed, these bands are of a nonchiral nature.

This work was supported by the 21st century center of excellence program for Tohoku University. G.R. acknowledges the support from BGNSF within contract VUF 06/05. N.P. thanks the support from the DFG under grant no. SFB 634. J.T.

TABLE IV. $B(M1)/B(E2)$ staggering pattern of the observed doublet bands for different configurations.

	Configuration	$I - I_0 =$ even	$I - I_0 =$ odd	I_0^π	
Odd-odd	$\pi h_{11/2} \otimes \nu {h_{11/2}}^{-1}$	Large	Small	9^+	^{124,126,128,130,132}Cs [3,8,9], ^{134}La [5]
Odd-odd	$\pi {g_{9/2}}^{-1} \otimes \nu h_{11/2}$	Large	Small	8^-	^{100}Tc [13], ^{104,106}Rh [10,11]
Odd-A	$\pi {h_{11/2}}^{2} \otimes \nu {h_{11/2}}^{-1}$	Small	Large	$\frac{25}{2}^-$	^{135}Nd [17]
Odd-A	$\pi {g_{9/2}}^{-1} \otimes \nu {h_{11/2}}^{2}$	Small	Large	$\frac{23}{2}^+$	^{103,105}Rh [12,14]

acknowledges the support from OTKA grant number K72566. R.W. acknowledges the support from UK EPSRC. This work is also supported by the U.S. Department of Energy, Office of Nuclear Physics, under contract no. DE-AC02-06CH11357.

[1] S. Frauendorf and J. Meng, Nucl. Phys. **A617**, 131 (1997).
[2] C. M. Petrache, D. Bazzacco, S. Lunardi, C. R. Alvarez, G. de Angelis, M. de Poli, D. Bucurescu, C. A. Ur, P. B. Semmes, and R. Wyss, Nucl. Phys. **A597**, 106 (1996).
[3] T. Koike, K. Starosta, C. J. Chiara, D. B. Fossan, and D. R. LaFosse, Phys. Rev. C **67**, 044319 (2003).
[4] A. A. Hecht, C. W. Beausang, K. E. Zyromski, D. L. Balabanski, C. J. Barton, M. A. Caprio, R. F. Casten, J. R. Cooper, D. J. Hartley, R. Krücken *et al*., Phys. Rev. C **63**, 051302(R) (2001).
[5] R. A. Bark, A. M. Baxter, A. P. Byrne, G. D. Dracoulis, T. Kibedi, T. R. McGoram, and S. M. Mullins, Nucl. Phys. **A691**, 577 (2001).
[6] S. Zhu, U. Garg, B. K. Nayak, S. S. Ghugre, N. S. Pattabiraman, D. B. Fossan, T. Koike, K. Starosta, C. Vaman, R. V. F. Janssens *et al*., Phys. Rev. Lett. **91**, 132501 (2003).
[7] A. A. Hecht, C. W. Beausang, H. Amro, C. J. Barton, Z. Berant, M. A. Caprio, R. F. Casten, J. R. Cooper, D. J. Hartley, R. Krucken *et al*., Phys. Rev. C **68**, 054310 (2003).
[8] S. Wang, Y. Liu, T. Komatsubara, Y. Ma, and Y. Zhang, Phys. Rev. C **74**, 017302 (2006).
[9] G. Rainovski, E. S. Paul, H. J. Chantler, P. J. Nolan, D. G. Jenkins, R. Wadsworth, P. Raddon, A. Simons, D. B. Fossan, T. Koike *et al*., J. Phys. G: Nucl. Part. Phys. **29**, 2763 (2003).
[10] C. Vaman, D. B. Fossan, T. Koike, K. Starosta, I. Y. Lee, and A. O. Macchiavelli, Phys. Rev. Lett. **92**, 032501 (2004).
[11] P. Joshi, D. G. Jenkins, P. M. Raddon, A. J. Simons, R. Wadsworth, A. R. Wilkinson, D. B. Fossan, T. Koike, K. Starosta, C. Vaman *et al*., Phys. Lett. **B595**, 135 (2004).
[12] J. Timár, P. Joshi, K. Starosta, V. Dimitrov, D. Fossan, J. Molnar, D. Sohler, R. Wadsworth, A. Algora, P. Bednarczyk *et al*., Phys. Lett. **B598**, 178 (2004).
[13] P. Joshi, A. Wilkinson, T. Koike, D. Fossan, S. Finnigan, E. Paul, P. Raddon, G. Rainovski, K. Starosta, A. Simons *et al*., Eur. Phys. J. A **24**, 23 (2005).
[14] J. Timár, C. Vaman, K. Starosta, D. B. Fossan, T. Koike, D. Sohler, I. Y. Lee, and A. O. Macchiavelli, Phys. Rev. C **73**, 011301(R) (2006).
[15] D. Tonev, G. de Angelis, S. Brant, S. Frauendorf, P. Petkov, A. Dewald, F. Dönau, D. L. Balabanski, Q. Zhong, P. Pejovic *et al*., Phys. Rev. C **76**, 044313 (2007).
[16] E. Grodner, J. Srebrny, A. A. Pasternak, I. Zalewska, T. Morek, C. Droste, J. Mierzejewski, M. Kowalczyk, J. Kownacki, M. Kisielinski *et al*., Phys. Rev. Lett. **97**, 172501 (2006).
[17] S. Mukhopadhyay, D. Almehed, U. Garg, S. Frauendorf, T. Li, P. V. M. Rao, X. Wang, S. S. Ghugre, M. P. Carpenter, S. Gros *et al*., Phys. Rev. Lett. **99**, 172501 (2007).
[18] C. M. Petrache, G. B. Hagemann, I. Hamamoto, and K. Starosta, Phys. Rev. Lett. **96**, 112502 (2006).
[19] H. Dejbakhsh, R. P. Schmitt, and G. Mouchaty, Phys. Rev. C **37**, 621 (1988).
[20] A. Dewald, P. Sala, R. Wrzal, G. Böhm, D. Lieberz, G. Siems, R. Wirowski, K. O. Zeil, A. Gelberg, P. von Brentano *et al*., Nucl. Phys. **A545**, 822 (1992).
[21] A. Lipski, G. Rainovski, N. Pietralla, and A. Dewald, Nucl. Instrum. Methods A **590**, 69 (2008).
[22] A. Dewald, S. Harissopulos, and P. von Brentano, Z. Phys. A **334**, 163 (1989).
[23] S. Y. Wang, S. Q. Zhang, B. Qi, J. Peng, Y. M. Yao, and J. Meng, Phys. Rev. C **77**, 034314 (2008).
[24] T. Koike, K. Starosta, and I. Hamamoto, Phys. Rev. Lett. **93**, 172502 (2004).